ARKIV FÖR FYSIK Band 19 nr 21

Communicated 7 December 1960 by MANNE SIEGBAHN and ERIK HULTHÉN

K- and *L*-electron capture probabilities and the decay energy of Pb^{203}

By LARS PERSSON and ZIEMOWID SUJKOWSKI[1]

With 6 figures in the text

ABSTRACT

K X-ray spectra in coincidence with the gamma rays from the first and the second excited states of Tl^{203} have been studied using scintillation techniques and an isotope-separated sample. The L_I/K capture ratio has been deduced and the decay energy calculated according to the theory of Brysk and Rose. The total electron capture decay energy has been found to be 817^{+12}_{-10} keV. Single spectra of the *L* and *K* X-rays have been measured and their ratio compared with theory. The Coster–Kronig yield $f_{L_I L_{III}}$ has been deduced. The half-life of Pb^{203} has been remeasured and found to be 52.1 ± 0.2 h. The log ft values for the decay to the first and the second excited states have been determined using known branching ratios.

I. Introduction

Considerable interest has recently been shown in collecting experimental data on the decay energies in β-interactions throughout the periodic system. There is a need of information for β-theory and also for various less direct applications, e.g. obtaining improved atomic masses, calculations on nuclear reactions, etc. While fairly accurate data are at present available for most of the nuclear species decaying by β^- or β^+ emission, there is still a considerable number of electron capture transitions whose decay energies are known very inaccurately or the available information is contradictory. Since the decay energy in electron capture (E.C.) is taken by the monoenergetic neutrino, the experimental determination of this energy represents a difficult problem. Only the higher order processes can be subjected to direct measurements. Several indirect methods suitable for particular isotopes have therefore been worked out.

Among the more common methods used for the determination of the E.C. decay energy one can mention: (1) measurement of the end point of the internal bremsstrahlung spectrum or of the continuous electron spectrum accompanying E.C.; (2) determination of the (p, n) reaction threshold for the nucleus to which the E.C. takes place; (3) consideration of "closed cycles"; the total decay energy Q can sometimes be calculated from Q-values of neighbouring isotopes.

---

[1] On leave from the Institute for Nuclear Research, Warsaw.

Another possibility is to deduce the decay energy from the measured ratios of capture from different electron shells. In the calculation of the Q-value one has to rely upon the theoretical ratios predicted by β-theory. Thus, for instance, in allowed transitions the ratio of the probabilities P_X for L_I and K capture is

$$\frac{P_{L_I}}{P_K}=\frac{L_{L_I}}{L_K}\left(\frac{q_{L_I}}{q_K}\right)^2, \tag{1}$$

where q_{L_I} and q_K are neutrino energies for capture from the corresponding shells given by the difference between the decay energy Q and the binding energy of the shell in the daughter nucleus. The decay functions L_i (as well as M_i and N_i) have been given in graphical form by Brysk and Rose [1]. The data in tabulated form, as read from the graphs, can be found in the Tables of Wapstra *et al.* [2]. Other theoretical studies which have been published lately on the E.C. probabilities are those of Band *et al.* [3, 4].

Experimentally the P_L and P_K values can be determined in the following ways. (a) Direct measurements of L/K X-ray or Auger-electron ratios. This is the only method available when the decay leads directly to the ground state. In general K and L fluorescence yields as well as Coster-Kronig transition probabilities must then be known. (b) The measurement of the ratio of K capture to total capture. This is possible when the electron capture proceeds to an excited state. Coincidence experiments can then be performed between the γ- and the K X-rays and the K capture branching can be determined for the decay to the level in question. If N_γ and $N_{\gamma K}$ are the single gamma ray and the K X-ray–gamma coincidence counting rates, respectively, then

$$N_\gamma = N\varepsilon_\gamma\Omega_\gamma,$$
$$N_{\gamma K}=N\varepsilon_\gamma\Omega_\gamma\varepsilon_K\Omega_K\omega_K P_K,$$

where N is the decay rate, ε is the detection efficiency, Ω is the solid angle and ω_K is the K fluorescence yield. Then

$$\frac{N_{\gamma K}}{N_\gamma}=P_K\omega_K\varepsilon_K\Omega_K. \tag{2}$$

In order to calculate the ratio P_{L_I}/P_K, the theoretical ratios of the capture from the higher shells must in general be used. A summary of the experimental techniques and experimental results on E.C. ratios has recently been given by Robinson and Fink [5].

II. Earlier work on Pb^{203}

The E.C. decay of ${}_{82}Pb^{203}_{121}$ to levels in ${}_{81}Tl^{203}_{122}$ has been the subject of several thorough investigations because of the vicinity of this nucleus to the magic numbers 82 and 126 and interest in the comparison with predictions from the shell model. The decay scheme seems to be well established [6]. Branching ratios and the conversion coefficients of the γ-transitions have been determined with good accuracy in several studies (see, e.g. Nijgh *et al.* [7] and references there). The spin and parity sequence $\frac{5}{2}+\rightarrow\frac{3}{2}+\rightarrow\frac{1}{2}+$ has been firmly established in a number of publications on directional correlations (e.g. Deutsch and Goldberg [8] and references there). The as-

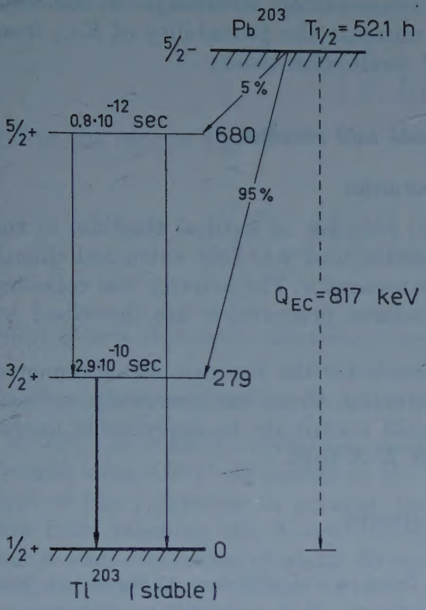

Fig. 1.

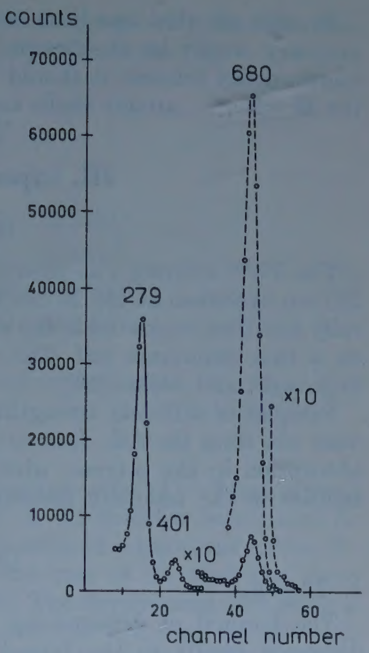

Fig. 2.

Fig. 1. Decay scheme of Pb^{203}.

Fig. 2. Gamma ray spectrum of Pb^{203} (background subtracted). A graded absorber consisting of 5 mm Pb + 3 mm Cd + thin sheets of Cu and Al was placed between the source and the $1\frac{3}{4}'' \times 2''$ NaI(Tl) detector. The dotted curve shows the result of a long-time run performed to search for the internal bremsstrahlung spectrum and new, faint transitions of energy above 680 keV (cf. IIIc). The 680 keV line has an intensity of 0.8 % of the 279 keV line [20].

signment $\frac{5}{2}-$ to the ground state of Pb^{203} was confirmed in many thorough investigations (see, e.g. Stockendal [9] and references there, and also Persson and Stockendal [10]). The spin of the ground state of Tl^{203} has been measured by Schuler and Keyston [11] in a study of the hyperfine structure of the atomic spectrum. The half-lives of the two excited levels have been studied with high precision in the work of McGowan and Stelson [12], Bashandy *et al.* [13] and Gorodetzky *et al.* [14]. Their findings are quoted in Fig. 1.

The data available to date on the decay energy of Pb^{203} are less satisfactory. Prescott [15] deduced the Q-value from K X-ray–gamma coincidence experiments with the 279 and 401 keV lines. He obtained the value $230\,^{+70}_{-40}$ keV for the decay to the 680 keV level and greater than 450 keV to the 279 keV level. The computations were based on the theory of Rose and Jackson [16] and of Marshak [17]. An estimate according to the closed cycle method yielded the total Q-value 800 ± 250 keV. Nijgh *et al.* [7] obtained the P_K value for the decay to the 279 keV level from the intensity ratio of K X-rays to 279 keV γ-rays. They have recalculated Prescott's values taking into account the probability of capture from the $M + N + \dots$ atomic shells according to the theory of Brysk and Rose [1]. Considering Prescott's and their own data they obtained 950^{+300}_{-70} keV as total Q-value.

In view of what has been said above, it was felt that a measurement of higher accuracy would be of interest. At the same time, taking advantage of the well-known decay scheme, it should be possible to estimate the probability of E.C. from the M + N + ... atomic shells and compare the result with theory.

III. Experimental methods and results

(a) *Source preparation*

The Pb^{203} activity was produced by a $(d, 2n)$ reaction on natural thallium in the 225-cm cyclotron at the Nobel Institute. The active lead was first extracted chemically and then separated in the magnetic isotope separator. The activity was collected on a thin aluminum foil. The details of the source preparation are described by Sujkowski and Melin [18].

Samples of different strengths and sizes, suitable for the separate measurements, were cut from the foil. Due to the isotope separation there was practically no self-absorption in the sources, which otherwise could contribute to appreciable uncertainties in the intensity measurements on soft L X-rays.

(b) *Coincidence spectra*

1. *Theory*

The method of determining the P_K value from a coincidence experiment was discussed briefly in the Introduction. The accuracy of a coincidence experiment with only one γ-transition is often impaired by uncertainties in the values of ω_K, ε_K and Ω_K entering formula (2). Moreover, the coincidence efficiency must then be known. These difficulties may be avoided in the case when two excited levels are fed in the electron capture decay.

Let us consider formula (1) and assume the result of Brysk and Rose that the ratio of L_I and K capture in allowed and first forbidden, non-unique transitions is nearly the same. For Tl $(Z = 81)$ we then have

$$P_K = 1 - 1.37\, P_{L_I} \tag{3}$$

deduced from the relations

$$\sum P_i = 1; \quad P_{L_{II}}/P_{L_I} = 0.080; \quad P_{L_{III}} \approx 0; \tag{4a}$$

$$(P_M + P_N + \ldots)/P_L = 0.270. \tag{4b}$$

Formula (1) gives in this case:

$$\frac{P_{L_I}}{P_K} = 0.152 \left(\frac{Q - 15.349}{Q - 85.531}\right)^2. \tag{5}$$

The binding energies and all numerical factors are here quoted according to Wapstra *et al.* [2].

Combining formulae (3) and (5) we obtain

$$P_K = \frac{1}{1 + 0.209 \left(\dfrac{Q - 15.349}{Q - 85.531}\right)^2}. \tag{6}$$

By measuring the ratios $N_{\gamma K}/N_\gamma$ for the γ-transitions to the ground state from the first and second excited states we can obtain, with help of formula (2),

$$\left(\frac{N_{\gamma K}}{N_\gamma}\right)_{\mathrm{I}} \Big/ \left(\frac{N_{\gamma K}}{N_\gamma}\right)_{\mathrm{II}} = \frac{P_K^{\mathrm{I}}}{P_K^{\mathrm{II}}},$$

and in the case of Pb^{203}:

$$\left(\frac{N_{\gamma K}}{N_\gamma}\right)_{279} \Big/ \left(\frac{N_{\gamma K}}{N_\gamma}\right)_{680} = \frac{1+0.209\left(\dfrac{Q-15.349}{Q-85.531}\right)^2}{1+0.209\left(\dfrac{Q+385.7}{Q+315.5}\right)^2}, \tag{7}$$

where Q now represents the decay energy to the second excited state.

2. *The experimental set-up*

A $1\frac{3}{4}'' \times 2''$ NaI(Tl) crystal was used as the γ-ray detector and a $1\frac{1}{2}'' \times 6$ mm crystal covered with 0.001″ Al served as the X-ray detector. A Cd absorber was placed in front of the γ-detector to prevent low energy, backscattered γ-rays and iodine X-rays from reaching the X-ray detector. A coincidence unit of the slow–fast type with a time-resolution of about 30 mμs was used [19]. The requirement of having a resolving time short enough to keep chance coincidences low and long enough with respect to the half-lives of the excited states (compare Fig. 1) was thus well fulfilled. The coincidence pulses were fed to the gate of a Wilkinson type 100-channel analyzer with a ferrite core memory and the coincident X-ray spectrum was recorded. K X-ray spectra in coincidence with the 279 and the 680 keV γ-lines are shown in Fig. 3. The solid angle subtended at the source by the X-ray detector was (45.7 ± 1.1) % throughout the experiments. Several geometries were tried with the γ-detector in different coincidence runs with the 279 keV line but no influence on the measured ratio was observed. In the measurements with the weak 680 keV line both solid angles could therefore be kept as large as possible.

The resolution of the γ-detector was about 9 % at 680 keV. The 279 and 401 keV γ-rays were clearly resolved and no contribution to the 279 keV line from the 401 keV line needed to be considered. Also the correction of the coincident X-ray spectrum due to the Compton distribution from the 401 keV line was estimated to be negligibly small.

3. *Experimental results*

Eleven and four independent coincidence runs were performed with the 279 and the 680 keV γ-lines, respectively. The number of coincidences under the peak was summed up for each run and the ratio $N_{\gamma K}/N_\gamma$ calculated. The straggling of the $N_{\gamma K}/N_\gamma$ values was well within the statistical errors. Table 1 gives the values obtained by adding the results of the separate runs for the 279 and 680 keV lines. The single counting rates are corrected for the background and the counting loss in the scaler. The coincidence background was very small. The correction for this effect was taken into account for the 279 keV line. A 0.4 % correction for the excess of K X-rays due to K-conversion of the 401 keV γ-rays was obtained from the known K conversion coefficient and branching ratio.

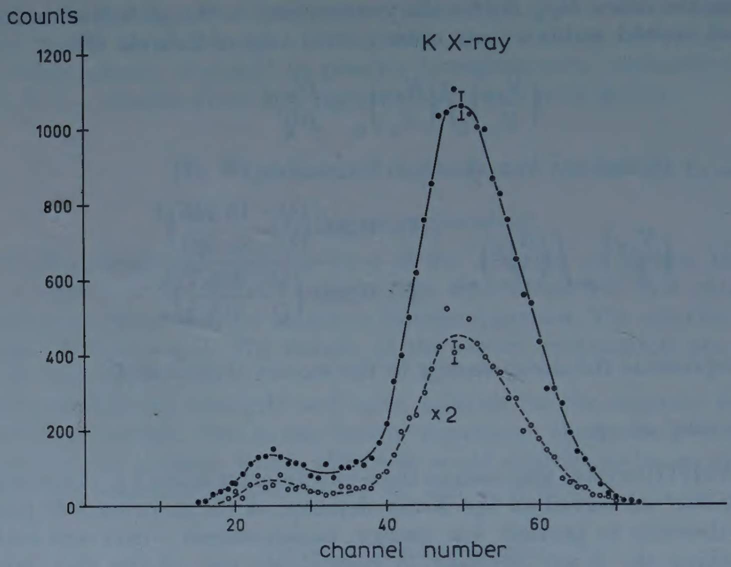

Fig. 3. *K* X-rays in coincidence with 279 and 680 (dotted curve) keV γ-rays (cf. IIIb).

From Table 1 we obtain

$$\left(\frac{N_{\gamma K}}{N_\gamma}\right)_{279} \Big/ \left(\frac{N_{\gamma K}}{N_\gamma}\right)_{680} = 1.69 \pm 0.07,$$

where the statistical error ± 0.05 was enlarged by taking into account the possible effect of changes of the coincidence efficiency over the measured region of the spectrum.

By solving equation (7) we obtain for the transition to the second excited state:

$$Q = 137 \pm 3 \text{ keV}.$$

Taking all numerical factors in the formulae with 10 % uncertainties we obtain $Q = 137 \pm^{9}_{8}$. Assuming the second excited level energy $E = 680\ ^{+3}_{-2}$, we finally arrive at

$$Q_{\text{total}} = 817\ ^{+12}_{-10} \text{ keV}.$$

Table 1. *K* X-ray coincidence spectra—experimental results.

Gamma ray (keV)	$N_{\gamma K}$	N_γ	$\frac{N_{\gamma K}}{N_\gamma}$
279	136 760 ± 400	488 152 ± 800	0.280 ± 0.002
680	7 930 ± 100	47 912 ± 400	0.165 ± 0.004

(c) *γ-ray spectrum*

The γ-ray spectrum was detected with a $1\frac{3}{4}'' \times 2''$ NaI(Tl) crystal with direct optical coupling to the photomultiplier (Harshaw integral line detector). The energy resolution for the Cs^{137} 662 keV γ-line was about 8 %. The γ-detector was placed in a special lead shield in order to decrease the background. A graded absorber of 5 mm Pb + 3 mm Cd + thin sheets of Cu and Al was placed between the source and the crystal to decrease *K* X-rays and 279 keV γ-rays relative to the 401 and the 680 keV rays. The spectrum obtained is shown in Fig. 2. A long-time run was also performed. The 680 keV γ-line has an intensity of 0.8 % of the 279 keV γ-line [20]. As one can conclude from the spectrum (Fig. 2), there is no indication of any γ-line with an energy greater than 680 keV. The limit that can be set is $\leqslant 2 \times 10^{-5}$ of the 279 γ-line intensity.

It can also be observed that there is no indication of an internal bremsstrahlung (I.B.) spectrum accompanying the E.C. above the 680 keV line. This is consistent with the *Q*-value measurement (cf. Section III b) and the assumption that the E.C. decay rate to the ground state is low (see Discussion). The end point of the I.B. spectrum for a *K* electron capture transition to the 279 level should be 452 keV, being masked by the Compton distribution of the 680 keV transition and the 279 and 401 keV lines. It was estimated that the I.B. spectrum for a transition to the 279 keV level should be observable in the above experiment for a total *Q*-value larger than 1400 keV (see theoretical work on the I.B. spectrum by Glauber and Martin [21]).

(d) *Single K and L X-ray spectra*

1. *Experimental determination of the K to L X-ray ratio*

The *K* and *L* X-ray spectra were measured with a $1\frac{1}{2}'' \times 6$ mm NaI(Tl) crystal covered with 0.001″ Al. The absorption cross-section of Al varies sharply with energy in the range of the *L* X-rays. The mean *L* X-ray energy was calculated from the estimated number of vacancies in different *L*-shells, assuming that the more prominent *L* X-transitions are the following: $L_2 \rightarrow M_1$, $L_2 \rightarrow M_5$, $L_3 \rightarrow M_1$, $L_3 \rightarrow M_4$, and $L_3 \rightarrow M_5$ [22]. The value obtained was 10.7 keV. The cross-section of Al for this energy is 22 ± 2 cm²/g [23]. Angular dependence was taken into account when calculating the absorption. The correction for absorption in air was about 15 % of the value for Al for a source–crystal distance of 35 mm and 5 % for a distance of 6 mm. The efficiency of the crystal was assumed to be 100 % for both *K* and *L* X-rays. The results as well as the corrections applied are listed in Table 2. An example of the spectra obtained is shown in Fig. 4.

Table 2. Experimental determination of the *K* to *L* X-ray intensity ratio.

Source-crystal distance (mm)	A_{KX}	A_{LX}	δ_1	δ_2	I_{KX}	I_{LX}	$\frac{I_{LX}}{I_{KX}}$
35 (series 1)	294 3 runs	97.6 4 runs	0.15 ± 0.03	0.013	294	112	0.38 ± 0.02
35 (series 2)	320 3 runs	104.6 3 runs	0.15 ± 0.03	0.013	320	124	0.39 ± 0.02
6	263 1 run	64.0 2 runs	0.23 ± 0.04	0.073	263	97.9	0.37 ± 0.02

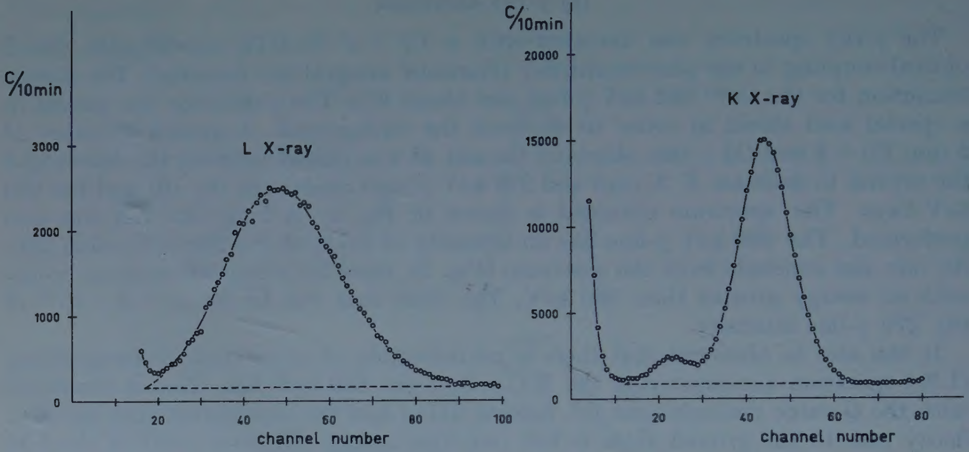

Fig. 4. X-ray spectra of Pb^{203}, measured with a $1\frac{1}{2}'' \times 6$ mm NaI(Tl) crystal covered with a 0.001″ Al foil. The L and K X-ray lines were measured separately at two different amplifier settings. The solid angle subtended at the 3 mm diameter source by the crystal was 5.5 %.

The following relationships were used:

$$I_{KX} = A_{KX}, \tag{8 a}$$

$$I_{LX} = A_{LX}(1 + \delta_1) + A_{KX} \cdot \delta_2, \tag{8 b}$$

$$\frac{I_{LX}}{I_{KX}} = 0.38 \pm 0.01, \tag{8 c}$$

where

A_{KX} and A_{LX} = areas below the K and L X-ray peaks, respectively, corrected for $T^1/_2$ and for the deadtime of the analyzer.
δ_1 = correction due to the absorption of the L X-rays in the Al cover of the crystal and in air.
δ_2 = correction due to the $K + L$ X-ray summing-up effect in the crystal.
I_{KX} and I_{LX} = intensities of the K and L X-rays, respectively.

2. *Deduction of the* $P_{M+N+\ldots}$ *value*

In order to compare the measured K/L X-ray ratio with theory, an estimate was made of the primary vacancies in the K and L atomic shells. The vacancies in the K shell are due to E.C. and internal conversion. In the L shell the primary vacancies are due to the above-mentioned processes as well as to the vacancy transfer from the K shell. Experimental values of relative γ-transition intensities and conversion coefficients have mainly been taken from Nijgh *et al.* [7]. The $L_I/L_{II}/L_{III}$ ratios for the conversion of the 279 keV line have been obtained from Fritsch [24] and the relative γ intensity and the K conversion coefficient of the 680 keV transition from Wapstra *et al.* [20]. Data on the number of primary holes in the L_i subshell caused by a K

Table 3. Contributions to the primary vacancies in the K and L atomic shells per one 279 γ-transition.

Atomic shell	Conversion of 279, 401 and 680 keV lines	E.C. decay to 279 keV level	E.C. decay to 680 keV level	f_{KL_i}	$K \to L_i$ transfers
K	$0.169 \pm 10\,\%$	$P_{K\,279} \cdot 1.174$	$P_{K\,680} \cdot 0.061$	—	—
L_{I}	$0.025 \pm 20\,\%$	$P_{L_{\text{I}}\,279} \cdot 1.174$	$P_{L_{\text{I}}\,680} \cdot 0.061$	0.03 ± 0.01	0.033
L_{II}	$0.015 \pm 20\,\%$	$P_{L_{\text{II}}\,279} \cdot 1.174$	$P_{L_{\text{II}}\,680} \cdot 0.061$	0.28 ± 0.01	$n_K \cdot 0.28$
L_{III}	$0.008 \pm 20\,\%$	0	0	0.50 ± 0.01	$n_K \cdot 0.50$

vacancy were taken from the tables of Wapstra *et al.* [2]. The total number of emitted L X-rays was then calculated according to formulae (9–10). The data are presented in Tables 3 and 4, where

$$\left.\begin{aligned} \nu_{L_{\text{III}}} &= \omega_{L_{\text{III}}} \\ \nu_{L_{\text{II}}} &= \omega_{L_{\text{II}}} + f_{L_{\text{II}}L_{\text{III}}} \cdot \omega_{L_{\text{III}}} \\ \nu_{L_{\text{I}}} &= \omega_{L_{\text{I}}} + f_{L_{\text{I}}L_{\text{II}}} \cdot \omega_{L_{\text{II}}} + (f_{L_{\text{I}}L_{\text{III}}} + f_{L_{\text{II}}L_{\text{III}}}) \cdot \omega_{L_{\text{III}}} \end{aligned}\right\} \tag{9}$$

$$\left.\begin{aligned} I_{KX} &= n_K \omega_K \\ I_{LX} &= \sum n_{L_i} \nu_{L_i} \end{aligned}\right\} \tag{10}$$

f_{KL_i} = number of holes in the L_i subshell caused by transitions to one hole in the K shell [2].
n_X = number of vacancies in the X-shell per one 279 keV γ-transition.
ω_X = fluorescence yield in the X-shell [2].
$f_{L_iL_j}$ = Coster–Kronig transition factors in the L-subshells [2].
ν_i = average number of L X-ray quanta emitted per primary vacancy in the L_i subshell.

Table 4. Number of K and L X-rays per one 279 keV γ-transition.

Atomic shell	n_X (From Table 3)	ω_X	ν_i	Coster–Kronig transitions	Intensity of X-rays
K	$P_{K\,279} \cdot 1.174 + 0.197$	0.955 ± 0.005	—	—	$I_{KX} = P_{K\,279} \cdot 1.122 + 0.188$
L_{I}	$P_{L_{\text{I}}\,279} \cdot 1.174 + 0.083$	0.08 $\pm 10\,\%$	0.34 ± 0.10	$f_{L_{\text{I}}L_{\text{II}}} = 0.12 \pm 50\,\%$ $f_{L_{\text{I}}L_{\text{III}}} = 0.68 \pm 20\,\%$ $f_{L_{\text{II}}L_{\text{III}}} = 0$	$I_{LX} = \Sigma I_{L_iX} = P_{L_{\text{I}}279} \cdot$ $\cdot\, 0.399 + P_{K\,279} \cdot 0.321 +$ $+\, 0.097$
L_{II}	$P_{K\,279} \cdot 0.330 + 0.087$	0.42 $\pm 10\,\%$	0.42 ± 0.04		
L_{III}	$P_{K\,279} \cdot 0.587 + 0.107$	0.31 $\pm 10\,\%$	0.31 ± 0.03	—	

Table 5. Number of K and L X-rays per one 279 keV γ-transition.

(Capture ratios assumed to be known).

p_{K279}	$p_{L_{\mathrm{I}}279}$	$\nu_{L_{\mathrm{I}}}$	I_{KX}	I_{LX}
0.785 ± 0.02	0.157 ± 0.02	$0.13 + 0.31\, f_{L_{\mathrm{I}}L_{\mathrm{III}}}$	1.061	$0.356 + 0.083\, f_{L_{\mathrm{I}}L_{\mathrm{III}}}$

From (8 c) and Table 4 we obtain:

$$\frac{P_{L_{\mathrm{I}}279}\, 0.399 + P_{K279}\ 0.321 + 0.097}{P_{K279}\, 1.122 + 0.188} = 0.38. \qquad (11)$$

From the coincidence measurement we have $P_{K279} = 0.785$ and eq. (9) may now be solved for $P_{L_{\mathrm{I}}}$. The value obtained is $P_{L_{\mathrm{I}}} = 0.14 \pm 0.05$. The main reasons for the big error in $P_{L_{\mathrm{I}}}$ are the large errors in $f_{L_{\mathrm{I}}L_{\mathrm{II}}}$, $f_{L_{\mathrm{I}}L_{\mathrm{III}}}$, and ω_{L_i}. These errors are estimated considering the disagreement in published experimental values [2, 5]. From the relationships (4 a) and $P_{L_{\mathrm{I}}} = 0.14 \pm 0.05$ we obtain $P_{M+N+\dots} = 0.07 \pm 0.05$. The theoretical value is 0.05 [2].

3. *Deduction of the Coster–Kronig yield* $f_{L_{\mathrm{I}}L_{\mathrm{III}}}$

The largest contribution to the error in the $P_{M+N+\dots}$ value, as determined in the preceding chapter, is due to uncertainties in the Coster-Kronig transition yields. It was therefore decided to estimate the factor $f_{L_{\mathrm{I}}L_{\mathrm{III}}}$, assuming the theoretical capture ratios as given by Brysk and Rose [1] for the Q-value 817 keV. Table 5 lists the values which were used in the calculations and which were not given in Tables 3 and 4. The intensities of the K and L X-rays are calculated according to the formulae (9–10).

From (8c) and Table 5 we obtain $f_{L_{\mathrm{I}}L_{\mathrm{III}}} = 0.57 \pm 0.10$. The main contributions to the error in $f_{L_{\mathrm{I}}L_{\mathrm{III}}}$ originate from the uncertainties in the values of ω_{L_i} and $f_{L_{\mathrm{I}}L_{\mathrm{II}}}$. From a graph given by Wapstra *et al.* [2] we obtain, for $Z = 81$, the value 0.68. Other references, quoted by the same authors, give the values 0.58, 0.68 and 0.52 for Z around 82.

(e) *Half-life measurement*

The decay of Pb^{203} was followed for 410 hours by measuring the intensity of the 279 keV γ-line with a $1\frac{3}{4}'' \times 2''$ NaI(Tl) integral line detector and a Wilkinson 100-channel pulse-height analyzer. A semilog plot of the intensity of the γ-line gave a straight line (Fig. 5). The decay data were analyzed by the method of least squares, the calculation being carried out on the electronic computer BESK. The value obtained was 52.1 ± 0.2 hours in agreement with measurements of Bartlett and Rebka [25]. The error is estimated from the diagram. Partial half-lives for the E.C. decay to the 680 and the 279 keV levels are 1050 ± 30 and 54.8 ± 0.5 hours, assuming a branching ratio to the 680 keV level of $(5.2 \pm 0.1)\,\%$ [7, 20].

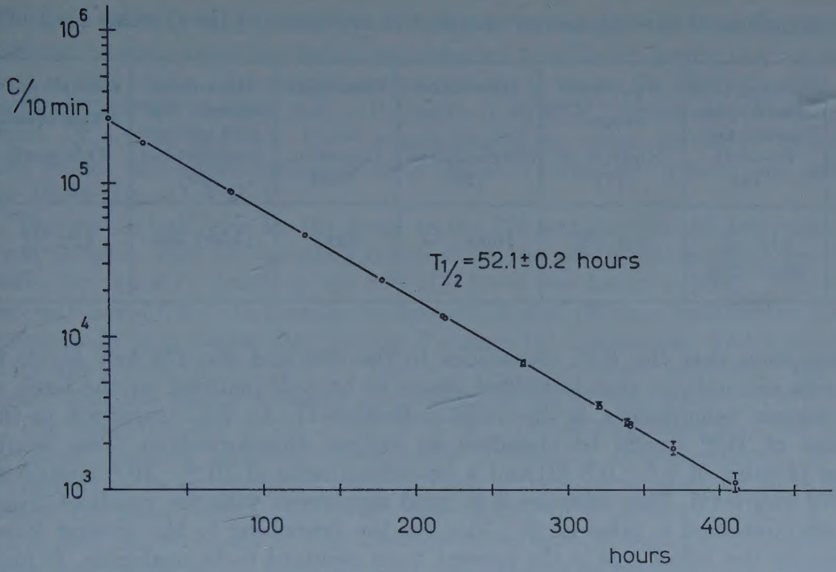

Fig. 5. Decay of Pb^{203}.

IV. Discussion

It should be emphasized that, in order to deduce the decay energy in the present work, we had to rely on the decay scheme. It is essential for the method that the character of the E. C. transitions to the levels in question is known.

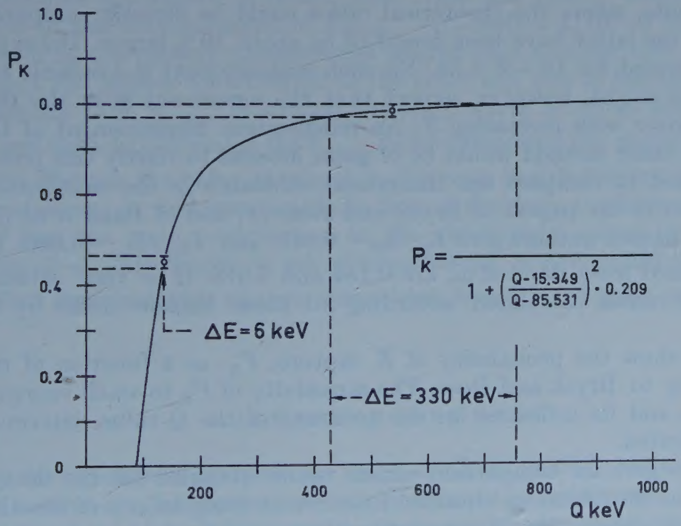

Fig. 6. Probability of K capture (P_K) versus E.C. decay energy (Q_{EC}) according to theoretical calculations by Brysk and Rose [1] for $Z = 81$. From the diagram one can see the difference in the uncertainty of the Q_{EC} values deduced from experimental P_K values for transitions to the 279 and 680 keV levels, respectively (cf. III b and IV).

Table 6. Comparison of various measurements and estimates of the Q-value for Pb^{203}.

Method and author	P_K coinc. (and closed cycle estimate) Prescott [15]	$\dfrac{N_{KX}\ \text{total}}{N_{\gamma 279}}$ Nijgh *et al.* [7]	Mass data Everling *et al.* [28]	Mass data Cameron [29]	Mass data (nuclear reaction energy compilation) [30]	$\dfrac{P_{K279}\ \text{coinc.}}{P_{K680}\ \text{coinc.}}$ This work
Q (keV)	910^{+70}_{-40} (800 ± 250)	950^{+300}_{-70}	1000 ± 70	1333	1100 ± 800	817^{+12}_{-10}

The assumption that the E.C. transitions to the 680 and the 279 keV levels in Tl^{203} are both non-unique, first-forbidden seems to be well justified on the basis of the decay scheme assignments, as discussed in Section II. An E.C. transition to the ground state of Tl^{203} should be classified as unique, first-forbidden. This would imply a log ft value of 8.5 ± 0.5 [2] and a branching ratio of $10^{-3} - 10^{-4}$ compared with the 279 keV level. This estimate is in good agreement with the result of Nijgh *et al.* [7], who obtained a value of $(0 \pm 3)\,\%$ for the branching to the ground level. A correction for this effect was in the present work assumed to be negligible. It may be added that a transition of higher intensity to the ground state would affect the results obtained from the single K and L X-ray spectra, while it should not have any influence on the Q-value deduced from the coincidence experiment.

In calculating the error of the Q-value (cf. IIIb) we have assumed in a rather arbitrary way 10 % uncertainties in the theoretical numerical factors entering the formulae. The validity of the results of Brysk and Rose for the electron capture ratios has recently been discussed in a review article by Robinson and Fink [5]. In six experiments, where the theoretical ratios could be directly compared to the measured ones, the latter have been found to be about 10 % larger. The experiments have been performed for $18 \leqslant Z \leqslant 53$. No such measurement is available for higher values of Z; one might, however, expect that the agreement with the theoretical values will improve with increasing Z. An independent measurement of the decay energy by some other method would be of great interest to clarify this point.

It is of interest to compare the theoretical constants in the calculation of P_K, as they are given in the papers of Brysk and Rose [1] and of Band *et al.* [3, 4]. For $Z = 81$ the first-named authors give $L_{L_{\mathrm{I}}}/L_K = 0.152$ and $L_{L_{\mathrm{II}}}/L_{L_{\mathrm{I}}} = 0.080$. The same quantities obtained from Band *et al.* are 0.154 and 0.078. It is very satisfactory to see that the Q-values calculated according to these authors differ by less than 0.5 keV.

In Fig. 6 we show the probability of K capture, P_K, as a function of the decay energy according to Brysk and Rose. The sensitivity of P_K to small energy changes at low Q-values and its influence on the accuracy of the Q-value determination is clearly demonstrated.

In Table 6 we give for comparison earlier values obtained for the decay energy of Pb^{203} as well as the estimates obtained from recent compilations of atomic masses. Large differences among the latter clearly illustrate a need of improved values of decay energies in this region.

Recently Gupta and Jha [26] have drawn attention to the fact that if one plots the decay energies of Hg–Tl isotopes versus neutron number according to systematics proposed by Way and Wood [27], a break at the neutron number 120 appears. It is difficult to state anything about the neighbouring Tl–Pb family in view of the scant data in this region. If, however, we assume the Q-values for Pb^{201} (β^+, EC), Pb^{205} (EC) and Pb^{207} ($Tl^{207}\beta^-$) to be $+3.5$, $+0.1$ and -1.45 MeV, respectively [6], then it is rather Pb^{203} ($N = 122$) and not Pb^{201} which shows an extra stability. Following Way and Wood, and interpolating between the above-mentioned data, one should obtain for Pb^{203} $Q \approx +1.8$ MeV.

The partial half-lives for the decay to the 279 and the 680 keV levels and the measured Q-value lead to the determination of the comparative half-lives. The log ft value for the E.C. decay to the 279 keV level was found to be 6.1 ± 0.1 and for the 680 keV level 6.2 ± 0.1 (graphs from Wapstra *et al.* [2] were used for the calculations). Empirically it is found that the log ft values for non-unique, first-forbidden transitions are within the limits 7 ± 1 (see, e.g. [2]). Our values are within this region and agree with the spin and parity assignment of the ground state of Pb^{203}.

The interpretation of the L and K X-ray spectra represents a rather complicated problem. Several auxiliary parameters concerning rearrangements in the inner electronic shells are required. Uncertainties in these parameters are large and directly affect the final results. Especially the variety of processes of filling a vacancy in an L-shell constitutes a serious obstacle. Some data on the mean L fluorescence yield have been given in the literature and compilations in the form of Z-dependent functions have been attempted ([2, 5] and references there). Strictly speaking, however, the concept of a mean L fluorescence yield has sense only for a particular decay, since the value $\bar{\omega}_L$ depends sharply on the distribution of primary vacancies in the L-subshells. In evaluating the data the partial fluorescence yields for the subshells, as well as the probability of vacancy transfers between the subshells (Coster–Kronig transitions), must therefore be considered. Unfortunately the accuracy with which these quantities are known is rather poor. This was clearly demonstrated by the large error in the determination of $P_{M+N+\dots}$ in Section IIId, in which the experimental error of the present measurement played only a minor role. It is interesting to note that the largest contribution to the error was due to the uncertainty in the Coster–Kronig yield $f_{L_I L_{III}}$. It seemed therefore worth while to turn the argument and use our data to determine the $f_{L_I L_{III}}$-factor, assuming the capture ratios as given by theory. Though the value obtained in this way is still subject to a considerable error, its accuracy is well comparable to that of the data available in the literature. It seems that the main contribution to the uncertainty comes from the errors in the values of ω_{L_i}. Obviously, a set of experiments, which would make possible an independent determination of these quantities, would be of great value.

ACKNOWLEGDEMENTS

We take this opportunity to express our sincere thanks to Professor Manne Siegbahn, head of the Nobel Institute, for the excellent working facilities put at our disposal.

The thanks of one of us (Z.S.) go also to "Syskonen Wesséns Stiftelse" for a maintenance grant and to the Institute of Nuclear Research in Warsaw for leave of absence.

Finally we want to thank Miss G. K. Oelsner, B. Sc., for correcting the English.

Nobel Institute of Physics, Stockholm 50, Sweden.

REFERENCES

1. Brysk, H., and Rose, M. E., Oak Ridge National Laboratory Rept. ORNL-1830 (1955) (unpublished), and Revs. Mod. Phys. *30,* 1169 (1958).
2. Wapstra, A. H., Nijgh, G. J., and Van Lieshout, R., Nuclear Spectroscopy Tables. North-Holland Publishing Co., Amsterdam 1959.
3. Band, I. M., Zyrianova, L. N., and Cin-Czen-Zuy, Izvest. Akad. Nauk S.S.S.R. Ser. Fiz. *20,* 1387 (1956).
4. Band, I. M., Zyrianova, L. N., and Suslov, J. P., Izvest. Akad. Nauk S.S.S.R. Ser. Fiz., *22,* 952 (1958).
5. Robinson, B., and Fink, R., Revs. Mod. Phys. *32,* 117 (1960).
6. Strominger, D., Hollander, J. M., and Seaborg, G. T., Revs. Mod. Phys. *30,* 785 (1958).
7. Nijgh, G. J., Wapstra, A. H., Ornstein, L. Th. M., Salomons-Grobben, N., Huizenga, J. R., and Almén, O., Nucl. Phys. *9,* 528 (1958/59).
8. Deutsch, B. I., and Goldberg, N., Phys. Rev. *117,* 818 (1960); see also Deutsch, B. I., thesis (unpublished).
9. Stockendal, R., Arkiv Fysik *17,* 579 (1960).
10. Persson, L., and Stockendal, R., Arkiv Fysik. *19,* 303 (1961).
11. Schuler, H., and Keyston, J. E., Z. Physik *70,* 1 (1931).
12. McGowan, F. K., and Stelson, P. H., Phys. Rev. *109,* 901 (1958).
13. Bashandy, E., Gerholm, T. R., and Lindskog, J., Arkiv Fysik *17,* 421 (1960).
14. Gorodetzky, S., Manquenouille, R., Richert, R., and Knipper, A., Compt. Rend. *251,* 65 (1960).
15. Prescott, J. R., Proc. Phys. Soc. London *67 A,* 254 (1954).
16. Rose, M. E., and Jackson, J. L., Phys. Rev. *76,* 1540 (1949).
17. Marshak, R. E., Phys. Rev. *61,* 431 (1942).
18. Sujkowski, Z., and Melin, O., to be published.
19. Johansson, B., Nucl. Instruments *1,* 274 (1957).
20. Wapstra, A. H., Maeder, D., Nijgh, G. J., and Ornstein, L. Th., Physica *20,* 169 (1954).
21. Glauber, R. J., and Martin, P. C., Phys. Rev. *104,* 158 (1956).
22. Siegbahn, M., Spektroskopie der Röntgenstrahlen. Verlag von Julius Springer, Berlin 1931.
23. McGinnies, R., X-ray Attenuation Coefficients from 10 keV to 100 MeV. National Bureau of Standards Supplement to Circular 583 (1960).
24. Fritsch, A. R., Ph.D. Thesis, UCRL-3452, June, 1956. As reported in Strominger, D., Hollander, J. M., and Seaborg, G. T., Revs. Mod. Phys. *30,* 785 (1958).
25. Bartlett, A. A., and Rebka, G., Bull. Am. Phys. Soc. Ser. II, *3,* 64 (1958).
26. Gupta, R. K., and Jha, S., Proc. International Conference on Nuclear Structure, Kingston, Canada 1960.
27. Way, K., and Wood, M., Phys. Rev. *94,* 119 (1954).
28. Everling, F., König, L. A., Mattauch, J. H. E., and Wapstra, A. H., Nucl. Phys. *18,* 529 (1960).
29. Cameron, A. G. W., A revised semi-empirical atomic mass formula with appended table of mass excesses and nuclear reaction energies. Atomic Energy of Canada Rept. CRP-690 and also Can. J. Phys. *35,* 1021 (1957).
30. Ashby, V. J., and Catron, H. C., Tables of Nuclear Reaction *Q* Values. UCRL-5419, 1959.

Tryckt den 13 april 1961

Uppsala 1961. Almqvist & Wiksells Boktryckeri AB